A fully automated, high-throughput electro-extraction and analysis workflow for acylcarnitines in human plasma and mouse muscle tissues

He, Y.; Miggiels, A.L.W.; Harms, A.C.; Rijksen, Y.; Brandt, R.M.C.; Vemeij, W.P.; ... ; Hankemeier, T.

Analytica Chimica Acta 1364 (2025) 344224

Contents lists available at ScienceDirect

Analytica Chimica Acta

journal homepage: www.elsevier.com/locate/aca

A fully automated, high-throughput electro-extraction and analysis workflow for acylcarnitines in human plasma and mouse muscle tissues

Yupeng He [a], Paul Miggiels [a], Amy Harms [a], Yvonne Rijksen [b,c], Renata M.C. Brandt [d], Wilbert P. Vermeij [b,c], Bert Wouters [a], Thomas Hankemeier [a,*]

[a] Metabolomics and Analytics Centre, Leiden Academic Centre for Drug Research, Leiden University, the Netherlands
[b] Princess Máxima Center for Pediatric Oncology, Utrecht, the Netherlands
[c] Oncode Institute, Utrecht, the Netherlands
[d] Department of Molecular Genetics, Erasmus MC Cancer Institute, Erasmus University Medical Center Rotterdam, Rotterdam, the Netherlands

HIGHLIGHTS

- A fully automated, high-throughput electro-extraction (EE) and analysis workflow was developed.
- High enrichment factors of up to 400 and extraction recovery of up to 99 % for acylcarnitines.
- 120 samples can be extracted and analyzed per day with cost of <0.1 Euro per sample.
- The workflow was successfully applied to human plasma and mouse muscle tissues.

GRAPHICAL ABSTRACT

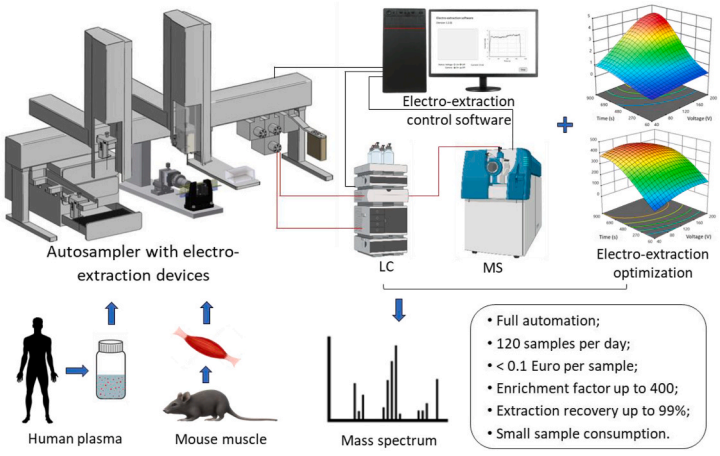

ARTICLE INFO

Keywords:
Electro-extraction
Automation
High-throughput
Sample-preparation
Bioanalysis
Sarcopenia

ABSTRACT

Background: The labor-intensive and time-consuming nature of sample preparation poses significant challenges for bioanalysis, especially for large-scale samples characterized by limited volumes/mass, and low analyte abundance. Additionally, manual sample processing can compromise reproducibility. To overcome these limitations, automation and high-throughput methodologies are essential, highlighting the need for an automated, high-throughput sample preparation and analysis workflow.

Results: This study presents a fully automated, high-throughput electro-extraction (EE) platform integrated with a CTC PAL3 autosampler and liquid chromatography–mass spectrometry analyzer. The integrated platform underwent qualification, followed by optimization of EE parameters using a Design of Experiment approach. Ten acylcarnitines were selected as model analytes. The optimization models exhibited strong fits ($p < 0.006$, $R^2 > 0.91$). The optimized platform achieved an enrichment factor of up to 400 (an extraction recovery of up to 99 %)

* Corresponding author. Einsteinweg 55, 2333 CC Leiden, the Netherlands.
E-mail address: hankemeier@lacdr.leidenuniv.nl (T. Hankemeier).

https://doi.org/10.1016/j.aca.2025.344224
Received 26 March 2025; Received in revised form 18 May 2025; Accepted 19 May 2025
Available online 20 May 2025

in designed academic samples, and was effectively implemented and evaluated using 20 μL of spiked human plasma samples. To test clinically relevant materials, the platform was utilized to study the effects of muscle tissue isolation speed on acylcarnitine stability, and to examine acylcarnitine abundance across muscle types in progeria (sarcopenia) mouse muscle. We found that the speed of muscle isolation does not affect measured levels of acylcarnitines, and detected higher acylcarnitine abundances are consistent with literature.

Significance: This study provides an automated, high-throughput, and cost-effective workflow enabling extraction and analysis of 120 samples per day, with a cost of <0.1 Euro per sample. It presents a significant stride towards the creation of fully-automated, high-throughput bioanalysis workflows for large-scale studies involving biomass limited samples in the foreseeable future.

1. Introduction

Sample preparation is a pivotal step in the bio-analytical workflow, including the extraction, enrichment, and removal of interferents from analytes. The manual approaches to sample preparation often encounter significant challenges, notably labor intensity and time consumption, especially when handling a high number of samples that are limited in mass/volume or have low analyte abundance [1–4]. Moreover, manual sample preparation can compromise reproducibility when analyzing numerous samples [5,6]. Addressing these challenges requires the exploration of alternative methodologies. This includes fully automated, high-throughput sample preparation techniques that can reliably purify and concentrate analytes from small-volume/mass and/or low abundance samples. Such methods should also reduce solvent usage and be directly coupled to analytical instrumentations, *i.e.*, liquid chromatography-mass spectrometry (LC-MS) or capillary electrophoresis-mass spectrometry [1,7–10].

Liquid-liquid extraction (LLE) and solid-phase extraction (SPE) have been predominant sample-preparation methods over the past decades [11–13]. However, these techniques are both labor and time-intensive, relying heavily on the use of significant amounts of environmentally unfriendly reagents. This often results in analyte dilution, especially for samples with limited volumes. Electro-driven extraction, where charged analytes migrate from the sample to the acceptor phase under an applied electric field, has garnered attention in recent years. Its appeal lies in its straightforward extraction process, minimal reagent and sample consumption, and high analyte enrichments [14–17]. There are two primary classifications of this method: supported liquid membrane electro-membrane-extraction (SLM-EME) and free liquid membrane electro-membrane-extraction (FLM-EME). The distinguishing factor between them is the presence of a solid membrane separating the sample and acceptor phase [17]. FLM-EME is a more cost-effective and readily automated option due to the exclusion of a solid membrane. Three-phase electro-extraction (EE) with an aqueous acceptor droplet generated in the organic phase is a subtype FLM-EME, was first performed on an automated nanoESI robot (Triversa NanoMate) by Raterink et al. [18]. A limitation of this setup was its offline coupling with separation and analysis instruments, which affected its analysis throughput and led to the injection of only a fraction of the extract [18]. We automated the three-phase EE by using a CTC PAL robotic autosampler with integration of a machine vision system and a well plate made of cyclic olefin copolymer (COC) selected due to its optical transparency (for the digital camera), chemical resistance to the reagents used, and good machinability [19]. However, the custom-designed well plate, measuring 98 × 16 × 6 mm, could accommodate only up to 3 samples due to the constraints of the commercial COC plate size (100 × 100 × 6 mm). Furthermore, the commencement of each new sample required manual repositioning of the well plate to facilitate syringe needle insertion into the correct sample, which does not fit with high-throughput sample preparation and analysis requirement.

Sarcopenia, an age-associated disease, manifests as diminished muscle mass and function, posing a significant global health concern [20,21]. Mice deficient in the multi-functional DNA excision-repair gene Ercc1 (*Ercc1*$^{\Delta/-}$) accumulate DNA damage in a time- and exposure-dependent manner, progressively compromising DNA function, including interfering with gene expression by physically stalling transcribing RNA polymerases. This so-called "transcription stress" leads to cellular functional decline, causing accelerated aging and numerous age-related pathologies and other features seen in natural aging [22–27]. These mice are widely used in the investigation of aging and age-related diseases, for example, sarcopenia [28–32]. As the *Ercc1*$^{\Delta/-}$ mice exhibit early cessation of growth, only small amounts (*i.e.*, 5–20 mg dry weight) of (skeletal) muscle can be collected. Acylcarnitines, *i.e.* acetyl-carnitine, decanoyl-carnitine, hexanoyl-carnitine, and lauroyl-carnitine, play important roles in fatty acids transport into mitochondria for energy production in muscle cells, and are highly associated with muscle strength and functioning. Raterink et al. optimized acylcarnitine extraction by an EE method [18]. However, an automated and high-throughput EE setup for acylcarnitines still needs to be developed, optimized, and applied to biological samples, *i.e.*, muscle tissues from progeria (*Ercc1*$^{\Delta/-}$) mice.

Therefore, in this study, a fully automated and high-throughput sample preparation platform, three-phase EE, was developed and integrated with an LC-MS analyzer. Three crucial EE parameters, *i.e.* ratio of formic acid (FA) in sample to acceptor phase, extraction voltage, and extraction time, and ten kinds of acylcarnitines, *i.e.* carnitine, acetyl-carnitine, propionyl-carnitine, isobutyryl-carnitine, valeryl-carnitine, hexanoyl-carnitine, octenoyl-carnitine, octanoyl-carnitine, decanoyl-carnitine, and lauroyl-carnitine, were utilized for the EE parameter optimization using an experimental design methodology (Box-Behnken design). The optimal platform was first evaluated using human plasma samples and the utility was then demonstrated on *Ercc1*$^{\Delta/-}$ mouse muscle tissues exhibiting sarcopenia mimicking a medically relevant setting to investigate the acylcarnitine abundance differences across muscle types, and whether immediate sample isolation (directly after mouse dissection) is necessary for acylcarnitine stability.

2. Material and methods

2.1. Chemicals

L-carnitine, acetyl-L-carnitine, DL-decanoylcarnitine, DL-hexanoylcarnitine, lauroyl-L-carnitine, isobutyryl-L-carnitine, DL-octanoylcarnitine, octenoyl-L-carnitine, propionyl-L-carnitine, valeryl-L-carnitine, and crystal violet were obtained from Sigma-Aldrich (Steinheim, Germany). MilliQ water was obtained from a Millipore high-purity water dispenser (Billerica, MA, USA). Formic acid and acetic acid were purchased from Acros Organics BVBA (Geel, Belgium). Ethyl acetate, methanol (MeOH) and acetonitrile were purchased from Biosolve Chimie SARL (Dieuze, France). All solvents were HPLC grade or higher.

2.2. Standard solutions and spiked plasma samples

All acylcarnitines were initially prepared in MeOH stock solutions at a concentration of 6.25 μg mL^{-1}. Standard solutions were prepared by diluting stock solutions to a concentration of 200 ng mL^{-1} in stated percentage of FA as academic samples. To evaluate the optimized EE

method, these standard solutions were also spiked to undiluted, 5-fold, and 10-fold diluted plasma samples with the final volume of 200 μL, both with and without protein precipitation (PP) procedures, maintaining a concentration of 200 ng mL^{-1}. For the PP process, plasma samples underwent protein precipitation using ice-cold MeOH at a ratio of 4:1 (MeOH: plasma, v/v) [33]. The resulting supernatant was then dried using a SpeedVac Vacuum concentrator (Thermo Savant SC210A, Waltham, Massachusetts, United States) and reconstituted at the stated percentage of FA in water to achieve 1-, 5-, and 10-times dilutions based on the initial volume. Human EDTA-treated plasma samples (Sanquin, Leiden, The Netherlands) were kept frozen at −80 °C until analysis and were thawed at room temperature directly before use.

2.3. Mouse muscle samples

Muscle tissues from mice deficient in the DNA excision-repair gene Ercc1 (*Ercc1*$^{\Delta/-}$) were utilized for the study on the effect of sample isolation speed on acylcarnitine stability including immediate and 15-min-delayed muscle collection. The generation and characterization of *Ercc1*$^{\Delta/-}$ mice have been previously described [23,24,31]. Commonly used muscle types for molecular analyses, gastrocnemius + soleus (Gas + Sol), quadriceps (Quadr), and extensor digitorum longus + tibialis anterior (EDL + TA), were collected from the hindlimbs of the animals. The dry weight of the collected muscle tissue ranged from 5.3 to 19.4 mg. More detailed information can be found in Supporting Information. Before the extraction by automated EE, the mouse muscle tissues were firstly lyophilized in a VaCo I freeze-dryer (Zirbus, Bad Grund, Germany; connected to an E2M12 high vacuum pump, Edwards, Crawley, England) for 24 h and weighed. Dry-homogenization in a Bullet Blender (BBX24; Next Advance, Averill Park, NY, USA) for 15 min at speed 9 with 100 mg (±10 %) zirconium oxide beads (0.5 mm; Next Advance, Averill Park, NY, USA) was used to process the freeze-dried tissue [34]. 200 μL formic acid solution (with optimum percentage) was added to Eppendorf tubes used for homogenization, then the solvent and muscle were moved to the designed 96-well plate for electro-extraction.

2.4. The automated, high-throughput EE setup

A CTC PAL3 RSI/RTC dual-headed robotic autosampler (CTC Analytics AG, Zwingen, Switzerland) was used for the automated EE platform as previously described [19]. Briefly, a 6-port VICI Cheminert Nanovolume vertical port injector valve was equipped with a 2 μL stainless steel loop (VICI AG, Schenkon, Switzerland) for sample injection; a drawer was used to store the samples (6 °C) (Fig. 1 A); a modified 10 μL syringe (CTC Analytics AG, Zwingen, Switzerland) (Fig. 1 B), a 0–1500 V DC high voltage power supply (RB10 1.5P, Matsusada

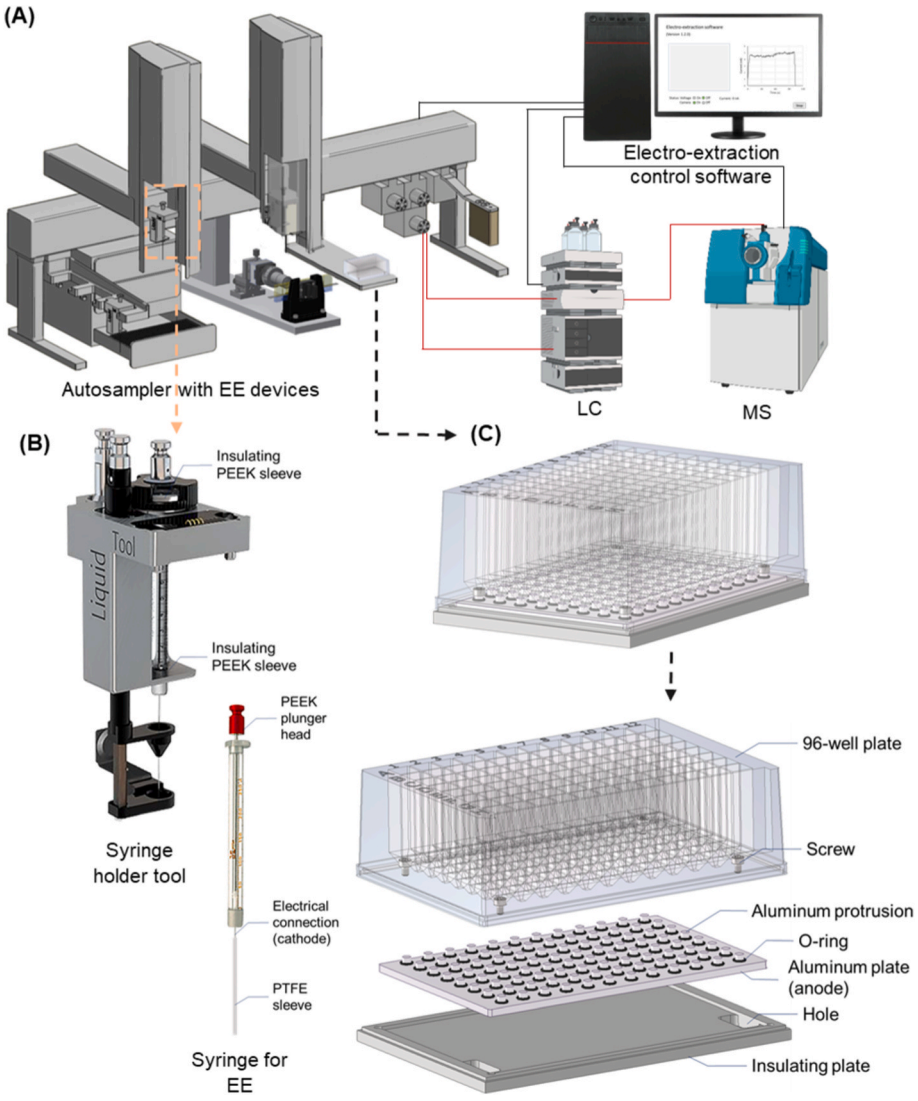

Fig. 1. Schematic diagram of the electro-extraction module integrated on the autosampler (A), modified syringe holder tool and syringe for EE (B), and details of the modified 96-well plate with a custom bottom electrode (C).

Precision, Shiga, Japan) and a custom 96-well plate (Fig. 1 C) were used for high-throughput EE process.

A 2.2 mL polypropylene 96-well plate (Ratiolab, Dreieich, Germany) was modified by cutting off the conical bottom part to form a 3 mm diameter circular hole in each well (Fig. 1C). An aluminum plate (116 × 74 × 2.4 mm) with 96 through-holes of 3.0 mm diameter was fabricated to be assembled with the modified 96-well plate. Ethylene propylene diene monomer (EPDM) O-rings 3 × 1 mm (ERIKS, Alkmaar Netherlands) were used for sealing the wells. EPDM O-rings were selected for their resistance to solvents and economic advantage. Four screws (2.8 mm diameter) and gaskets were used for assembly stability. Nuts fitting the screw size were fabricated in four positions in the corners of the aluminum plate. A polyether ether ketone (PEEK) plate (127.4 × 85 × 6 mm) was fabricated and attached to the bottom of the aluminum plate to insulate the electrode from the autosampler. Two holes in the PEEK plate were used for the power cable connection with the aluminum plate (Fig. 1C). All custom parts were designed and manufactured by the Fine Mechanical Department at Leiden University.

The EE process was controlled using an in-house developed LabView software (LabView 2021, National Instruments, Austin, Texas, USA). The CTC PAL3 autosampler was programmed and controlled with PAL Sample Control (PSC) 3.10 (CTC Analytics AG, Zwingen, Switzerland). An NI USB-6008 interface (National Instruments, Austin, Texas, USA) was utilized to synchronize with the autosampler via start/stop signals, supply 0–5V control signal to the power supply, and monitor the process current. Essential parameters for the EE process, *i.e.*, droplet volumes, extraction voltage, and extraction time, were input into the PSC sample list and communicated to the LabView software via a plaintext file.

2.5. Electro-extraction process

All the solvents and samples were stored at 6 °C within the autosampler drawer. At the start of sample analysis, the autosampler's left head, using a 1000 μL glass syringe (CTC Analytics AG, Zwingen, GmbH), separately transported 200 μL of samples and 250 μL of MilliQ water-saturated ethyl acetate from vials in the drawer to the 96-well plate for electro-extraction. Following each sample/solvent transfer, the 1000 μL syringe underwent cleaning with MeOH and water, performed thrice each. Then EE was applied by a modified 10 μL syringe on the autosampler right head as previously described [19]. A 0.5 μL acceptor droplet formed at the syringe needle tip after it was lowered into ethyl acetate in the well. The EE occurred at the set voltage and time, and the acceptor droplet was aspirated and injected in the valve for the LC-MS analysis. The 10 μL syringe was then cleaned with MeOH and water 3 times each. This workflow would then continue automatically until finishing all samples analysis. For muscle tissue extraction, 250 μL of MilliQ water-saturated ethyl acetate was transferred to the 96-well plate containing the formic acid homogenized muscle samples by the autosampler left head with a 1000 μL glass syringe. The extraction process was the same as described above. LC-MS methods for analyzing acylcarnitines were detailed in SI.

2.6. Data analysis and calculation

RStudio (Version April 1, 1106) and R (Version 4.0.5) were used for MS data analysis. Design-Expert (version 12.0, Stat-Ease, Minneapolis, USA) was utilized for the optimization of the parameters of the three-phase EE by using a Box-Behnken design (BBD) of experiment. The enrichment factor (EF) [15,18,35] and extraction recovery (ER) [15,36] were calculated by equations (1) and (2):

$$EF = [Acceptor\ phase]_{\ after\ EE} \Big/ [Aqueous\ sample]_{\ before\ EE} \quad \text{(Equation 1)}$$

$$ER(\%) = EF \times V_d/V_s \cdot 100\% \quad \text{(Equation 2)}$$

where V_d and V_s are the volumes of the acceptor droplet (0.5 μL) and aqueous sample (200 μL), respectively.

The limits of detection (LODs) were determined using a reported method based on the calibration curve and regression analysis of theoretical versus measured concentrations [37]. The peak area of acylcarnitines were normalized by the muscle dry weight, and statistically analyzed for further study.

3. Results and discussion

3.1. Qualification of the integrated EE-CTC system

The qualification of the EE-CTC system was conducted by assessing the modified syringe performance, automation workflow, and integrated software for controlling electro-extraction.

The modified syringe's performance was assessed through injection repeatability and carry-over tests using acylcarnitine standards (200 ng mL^{-1}) in partial-loop (1.0 μL, 1.5 μL) and full-loop (a 2.0 μL loop) injections. Following each acylcarnitine injection, three blank samples (MilliQ water) were processed, and this sequence was repeated five times. The relative standard deviation (RSD) was <10.3 % for 1.0 μL, <9.2 % for 1.5 μL, and <8.4 % for full-loop injections (Table S1). To minimize potential loss of the 0.5 μL acceptor droplet in the 2.0 μL loop, the 1.5 μL partial-loop injection was selected for further experiments. Additionally, carry-over was <4.4 %, confirming the syringe's suitability for both partial- and full-loop injections. The automation workflow and software integration were assessed by executing a complete electro-extraction and analysis process. This included: (1) transferring test samples (1000 ng mL^{-1} crystal violet) and organic solvents from vials in the CTC drawer to a 96-well plate using a 1000 μL syringe on the CTC's left head, (2) loading the acceptor solvent into the modified syringe for EE, (3) preparing for EE by forming an acceptor droplet in the organic solvent, (4) initiating EE with the predefined voltage and extraction time, (5) recording the EE current, (6) stopping EE, (7) triggering and stopping the LC-MS system for data acquisition, and (8) cleaning the syringes and preparing for the next sample. The successful extraction of crystal violet under the applied voltage and extraction time (Fig. S1), and EE current monitoring at varying voltages and formic acid concentrations (Fig. S2), demonstrates successful integration and precise control of the electro-extraction process. These results confirm the reliability of the modified syringe, automation workflow, and integrated software in enabling electro-extraction.

3.2. Model for EE parameter optimization

Box-Behnken design (BBD) was utilized to optimize the parameters of the automated EE setup for achieving a maximum enrichment factor for the ten acylcarnitines. Based on previous electro-driven extraction studies [35,38,39] and the following theoretical model of the analytes flux (J_i) [40–42], three pivotal parameters, the ratio of FA in sample to acceptor phase (A), applied voltage (B), and extraction time (C), were selected for simultaneous optimization to achieve a higher J_i (Equation (3)).

$$J_i = -D_i / h \cdot (1 + \nu / Ln\,\chi) \cdot (\chi - 1) / (\chi - exp(-\nu)) \cdot (C_{ih} - C_{i0}\ exp(-\nu)) \quad \text{(Equation 3)}$$

In Equation (3), i indicates the i th cationic substance; D_i is the i th ion diffusion coefficient; h is the membrane thickness; C_{ih} and C_{i0} are the concentration of i th cationic substance in the sample solution and the acceptor phase; ν is a dimensionless driving force which is related to the applied electrical potential/voltage; χ the ion balance, *i.e.*, the ratio of the total ionic concentration in the sample to that in the acceptor phase. Increasing the applied voltage (increasing ν) or decreasing the ion balance (χ) was reported to be helpful for improving J_i [42].

Quadratic models were utilized in BBD and 17 experiments were conducted in triplicate for the optimization. Various concentrations of

FA were tested both in the acceptor phase (0.5 % and 2.0 %) and the academic sample (0.2 %, 2.0 %, and 3.8 %) to investigate the effect of FA ratio between the sample and acceptor phase on the enrichment factor of acylcarnitines, and listed in Table S2, respectively, for acceptor phase with 2.0 % and 0.5 % FA. The optimization range for voltage (40–200 V) was defined by system limitations, while the extraction time (60–900 s) was based on both literature precedent [18] and the voltage range selected for this study. The maximum voltage, 200 V, was determined by the acceptor droplet stability for at least 900 s (Fig. S3) using the EE machine vision setup described in Ref. [19]. The 40 V represents the minimum voltage at which the extracted analytes can still be reliably detected. 1000 ng mL^{-1} of crystal violet was spiked in the academic sample to allow the acceptor droplet to be easier visualized by camera. A long extraction time, 900 s, was conducted for the determination based on a previous acylcarnitine electro-extraction study [18], and the antagonistic relationship between extraction time and applied voltage—where lower voltage requires a longer extraction time to achieve optimal enrichment, and vice versa.

The developed quadratic models were all significant ($p < 0.02$), and the lack of fit of these models was insignificant ($p > 0.06$) for all acylcarnitines in acceptor phase with 2.0 % FA (Table S3) and 0.5 % FA (Table S4), indicating good fit of the developed models with the parameters used for acylcarnitine electro-extraction optimization. The models' determination coefficients, R^2 (exceeding 0.91 for 2.0 % FA and 0.87 for 0.5 % FA acceptor phases) and adjusted R^2 (>0.80 for 2.0 % FA and >0.71 for 0.5 % FA acceptor phase), also revealed the good fit of models regardless of the model compounds (Table S3 and Table S4). Overall, the developed models fit well with subsequent automated EE optimizations.

3.3. EE parameter optimization

Models corresponding to the acceptor phases of 2.0 % FA and 0.5 % FA were individually optimized. The optimal enrichment factors of all acylcarnitines in these two acceptor phases were compared to determine a better ratio of FA in sample to acceptor droplet for the developed EE method. Table S5 indicates a notably higher optimized EF in the acceptor phase with 2.0 % FA than in the one with 0.5 % FA. For the acceptor phase containing 2.0 % FA, the optimal EF of all acylcarnitines was obtained at a 1.25 ratio of FA in sample to acceptor phase (2.5 % FA in sample), extraction voltage of 175 V, and extraction time of 693 s (Fig. 2 and S4). The current of the optimized automated EE method was monitored in Fig. S6A. During electro-extraction of all acylcarnitines, the acceptor droplet acts as the cathode, where the pH increased with electrolysis, leading to a shift in charge state equilibrium, polarity and solubility of all acylcarnitines in acceptor droplet, which has been largely reported in previous electro-driven extraction studies [14,18,35,43–45]. A higher FA percentage in acceptor phase slows down the pH increase during EE, resulting in less back extraction of acylcarnitines into the organic phase, and higher enrichment factors in the acceptor phase. A higher percentage of FA in aqueous samples boosts buffer capacity, ensuring a more consistent pH during EE. However, the EF of all acylcarnitines decreased when the FA percentage was greater than its optimal value in the sample; 2.5 % (the FA ratio was 1.25). Similar

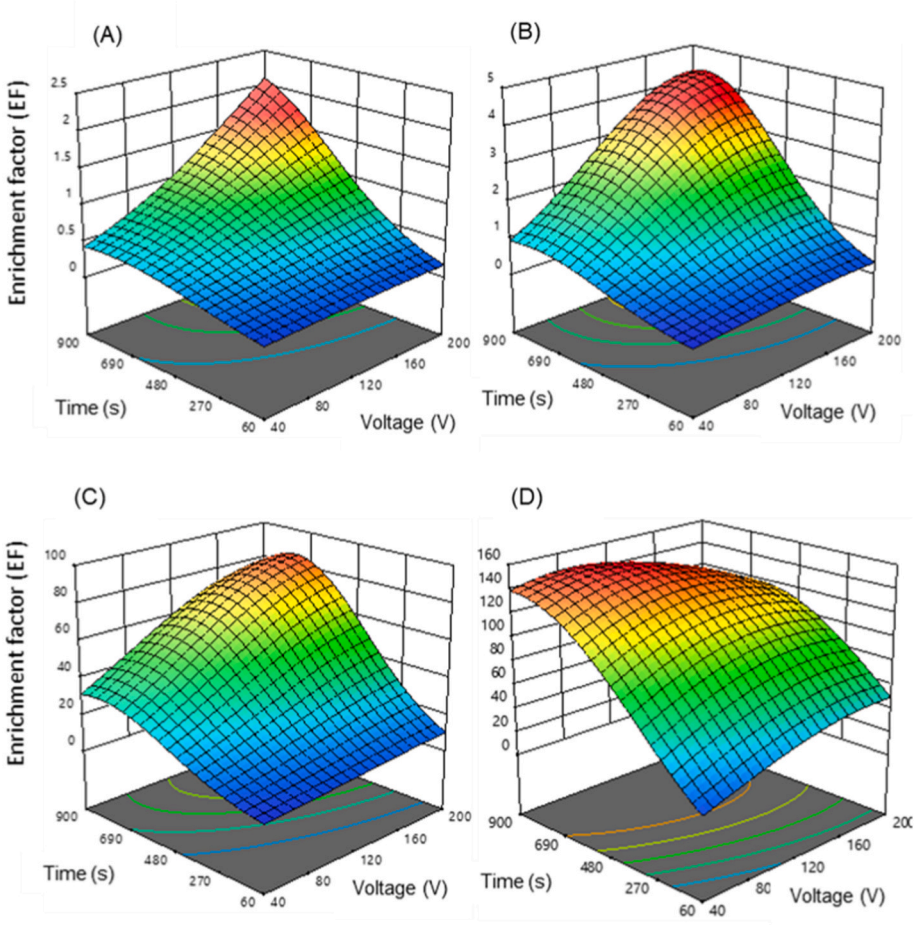

Fig. 2. Surface profiles of four representative developed quadratic models for carnitine (A), acetyl-carnitine (B), hexanoyl-carnitine (C) and octenoyl-carnitine (D), as function of electro-extraction time (x-axis) and extraction voltage (y-axis) at the optimum formic acids 2.5 % in sample, and 2.0 % in acceptor droplet. Models for all acylcarnitines can be found in Fig. S4.

results of a declining trend in the enrichment factor after the FA percentage (or FA ratio of sample to acceptor phase) reached the optimal values were also observed by Nojavan et al. and our previous study [19,46]. This may be due to the lower electric field, increased electrolysis during electro-extraction, and a too high ion balance (χ in Equation (3)) induced by the high ionic concentration in the sample solution at these conditions [44,47].

Both the migration of charged acylcarnitines during EE and the extraction efficiency can be improved by higher extraction voltage. However, for voltages greater than the optimal value, 175 V, the EF of several acylcarnitines, *i.e.*, acetyl-carnitine, decanoyl-carnitine, lauroyl-carnitine, isobutyryl-carnitine, octenoyl-carnitine, propionyl-carnitine, and valeryl-carnitine, decreased. Similar results of reduced EF at voltage over the optimal value were also reported by Schoonen et al. [48], Nojavan et al. [46,49], and our previous report [19]. Simultaneously, the same declining trend of EF was also observed in extraction time after reaching the optimal value, 693 s. These declining EF trends during method optimization may be explained by the excessive electrolysis in the acceptor phase [44,45,50,51], the shift charge state, reduced polarity, and increased back extraction of these acylcarnitines into the organic phase, which has been observed in numerous previous studies [14,18,35,43–45]. This antagonistic effect between extraction time and voltage was also consistent with the theoretical model of analyte flux (J_i) in Equation (3) [41].

The enrichment factor of the acylcarnitines is closely tied to their polarities, represented by the log P value (Fig. 3). More polar analytes yield lower EFs, *i.e.*, carnitine (log P = −4.9, EF = 1.5), acetyl-carnitine (log P = −4.4, EF = 4.0), and propionyl-carnitine (log P = −3.3, EF = 10.0). Decanoyl-carnitine and lauroylcarnitine reached nearly the maximum EF (400) with the highest log P values, *i.e.*, −0.63 and 0.26, respectively. A similar EF trend with analyte polarity was also observed in Raterink et al.'s study [18]. The much higher enrichment factors of some acylcarnitines, *i.e.*, lauroylcarnitine (397), decanoylcarnitine (393) and octanoylcarnitine (246), in our study compared to Raterink et al.'s results (<25) may be due to the implementation of a smaller acceptor droplet (0.5 μL versus 2.0 μL) and a higher optimal extraction voltage (175 V versus 140 V) [18]. The extraction time and recovery were comparable with Raterink et al.'s EE method [18].

3.4. Bio-fluid application to human plasma and EE-CTC system performance evaluation

To further investigate the optimized and fully-automated EE setup for biological samples, ten acylcarnitine standards were spiked into various human plasma samples – undiluted, 5-fold diluted, and 10-fold diluted, both with and without protein precipitation (with an addition of 2.5 % FA). Significantly ($p < 0.05$) higher EFs for several acylcarnitines, *i.e.*, acetylcarnitine, hexanoylcarnitine, lauroylcarnitine, isobutyrylcarnitine, octenoylcarnitine, propionylcarnitine, and valerylcarnitine, were observed in 10-fold (or 5-fold) diluted plasma, in contrast to undiluted samples without PP. This suggests that dilution mitigates matrix effects and improves automated EE performance in plasma samples (Fig. 4 and S5). A plausible reason may be that dilution decreases the quantity of plasma proteins at the interface between the sample and organic layer, minimizing potential protein barriers to analyte migration, and thus, improving extraction efficiency. Similar results were also reported and observed for basic compound extraction [19,35,52]. Hence, high protein concentrations in biological samples may be an important confounder for this type of extraction. For most acylcarnitines, the EFs in plasma samples with PP were significantly ($p < 0.05$) diminished compared to those without PP, possibly due to analyte loss during the PP procedure (Fig. 4 and S5). Even though the EF of acylcarnitines in plasma samples was smaller than in academic samples (Table S5), the values were much larger than in the previous acylcarnitine electro-extraction study in plasma [18], demonstrating the improved extraction efficiency of the optimized EE setup for acylcarnitines.

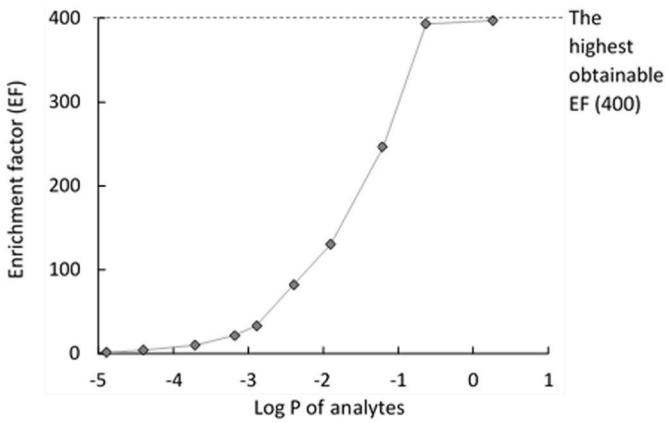

Fig. 3. The optimal enrichment factor versus log P of all model acylcarnitines.

The automated EE setup was further characterized by determining the response function, repeatability, limits of detection (LODs), limits of quantification (LOQs), and accuracy before its application in muscle tissues (Table 1). The optimal extraction conditions that yielded the highest enrichment factor, *i.e.*, 10-fold diluted plasma without PP, were utilized for the evaluation. The good linear response ($R^2 > 0.99$) within the concentration range of 10–1000 ng mL^{-1}, low LODs (<25.8 pg mL^{-1}) and LOQs (82.2 pg mL^{-1}), high accuracy value (89–112 %), acceptable intra- and inter-day relative standard deviation (RSD) (<18 %) of ten kinds of acylcarnitines demonstrated the stability, sensitivity, and repeatability of the automated EE setup in plasma samples. With its 24/7 operational capacity, the workflow enables the extraction and analysis of 96–120 samples per day for acylcarnitines, based on the time required for each step of the EE procedure, including sample and solvent loading, syringe cleaning, and preparation for the next sample. The cost is less than 0.1 Euro per sample, including all solvents and the consumable 96-well plate (detailed costs can be found in Table S6). With its 24/7 operational capability, the throughput of our developed workflow exceeds that of previously reported methods, including supported liquid membrane electro-membrane extraction (SLM-EME) [53], continuous-flow EME [48], other free liquid membrane EME (FLM-EME) approaches [18,54], as well as manual [55] and semi-automated solid-phase extraction (SPE) methods [56]. For instance, the semi-automated SPE method, applied to plasma samples after deproteinization, achieved a throughput of approximately 8 min per sample, not including time for sample loading and protein precipitation. The repeatability (RSD <18 %) and accuracy (84–116 %) of these reported methods are generally comparable to our workflow. However, the semi-automated SPE method (<7.8 %) and continuous-flow EME (<8.1 %) demonstrated better repeatability due to internal standard correction [48,56]. In terms of per-sample cost, SPE, SLM-EME, and continuous-flow EME methods may be relatively expensive due to the need for cartridges, membrane supports, or chip-based flow systems. FLM-EME methods offer lower per-sample costs due to utilizing only small volumes of solvents during extraction [18,54]. However, their throughput is limited by manual handling steps required during the extraction and analysis workflow, such as sample loading, solvent addition, container transfer, voltage application, sample injection, and LC-MS method initiation and termination (Table S7).

In the automated EE setup, the current during electro-extraction of bio-fluid samples was also recorded, and the results of samples that yielded the highest enrichment factor, *i.e.*, 10-fold diluted plasma is shown in Fig. S6B and S6C. A relatively stable current was observed in academic (Fig. S6A) and plasma samples with PP (Fig. S6C), which was similar to our previous observation [19]. The increasing current in plasma sample without PP up to 200 s (Fig. S6B) may be due to the decreased solvent conductivity, increased Joule heating, and increased

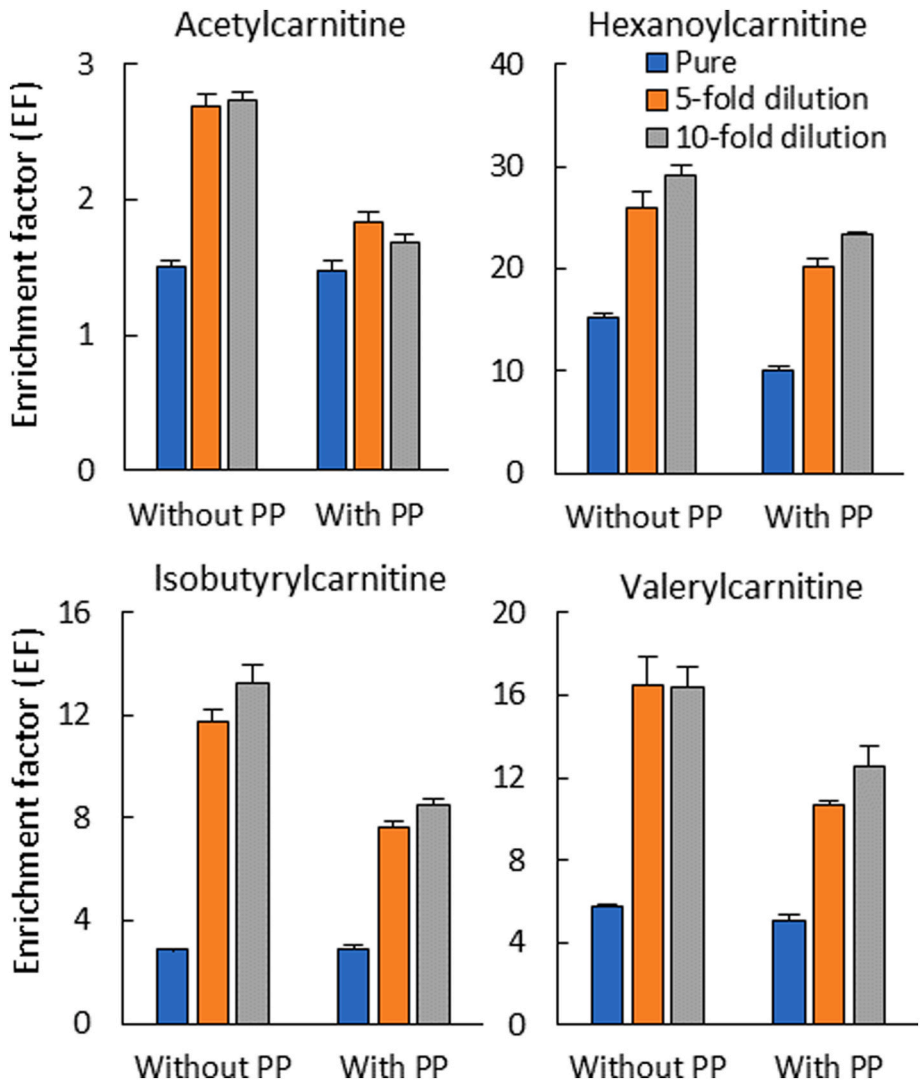

Fig. 4. The EF of four representative acylcarnitines spiked in pure, 5-fold, and 10-fold diluted plasma samples with and without protein precipitation (PP) (n = 3). The EF for all acylcarnitines can be found in Fig. S5.

Table 1
Calibration curve and precision (RSD) of the model compounds in diluted plasma samples by using the optimized EE method (n = 3).

	Linear range (ng mL^{-1})	R^2	LODs (pg mL^{-1})	LOQs (pg mL^{-1})	Accuracy (%) (50 ng mL^{-1})	RSD (50 ng mL^{-1})	
						Intraday	Interday
Carnitine	10–1000	0.995	3.9	13.0	102	8.10 %	11.51 %
Acetylcarnitine	10–1000	0.990	25.8	85.2	91	2.09 %	12.89 %
Propionylcarnitine	10–1000	0.994	6.7	22.1	101	6.18 %	10.34 %
Isobutyrylcarnitine	10–1000	0.991	7.8	25.6	102	11.91 %	9.66 %
Valerylcarnitine	10–1000	0.991	13.5	44.5	91	17.95 %	14.99 %
Hexanoylcarnitine	10–1000	0.990	11.2	37.0	89	16.69 %	12.47 %
Octenoylcarnitine	10–1000	0.995	3.0	9.8	112	4.41 %	3.75 %
Octanoylcarnitine	10–1000	0.998	6.5	21.5	91	9.97 %	16.63 %
Decanoylcarnitine	10–1000	0.996	5.5	18.2	96	5.82 %	12.31 %
Lauroylcarnitine	10–1000	0.993	4.2	13.7	107	16.02 %	17.12 %

temperature induced by proteins. This aligns with Babu et al.'s observation regarding increased protein concentration leading to reduced sample conductivity [57], and Gjelstad et al.'s report that increased temperature results in increased current during electro-extraction [42]. A slowly decreasing and stable current after 200 s in plasma sample without PP may be due to the heat exchange between EE solvents and the environment, which results in a slightly decreasing and then stable temperature of the solvents for EE.

3.5. Biological tissue application to mouse muscle tissues to study sample isolation speed on acylcarnitine stability and acylcarnitine abundance across muscle types

To deduce the effect of sample collection speed on the stability of these acylcarnitines, we assessed their abundance in both immediate and delayed-collected muscle tissues. Three specific muscle specimens were analyzed, namely the combined lower hindlimb muscles of

gastrocnemius and soleus (Gas + Sol), extensor digitorum longus with tibialis anterior (EDL + TA), and the upper hindlimb muscle, quadriceps (Quadr), which are frequently used mouse muscles for molecular analyses. A Partial Least Squares Discriminant Analysis (PLS-DA) was conducted to analyze the effects of muscle isolation speed on acylcarnitine stability in the three types of muscle tissues. The PLS-DA results showed no clear differences between immediate and 15-min-delayed isolated Gas + Sol, EDL + TA, and Quadr muscles (Fig. 5A–C). T-test analysis (with FRD correction) also revealed no significant difference ($p < 0.05$) for all the acylcarnitines (Table S8), demonstrating muscle collection speed does not affect the acylcarnitine levels in these various muscle specimens. This may be due to the stable properties of these acylcarnitines and/or enzymatic inactivity of the tissue at room temperature [58].

The optimized EE method was also applied to investigate differences in acylcarnitine abundance across muscle types. Notably, Quadr exhibited clear distinctions compared to the other two muscle specimens (Gas + Sol and EDL + TA) (Fig. 5D). To further explore these differences, a *t*-test analysis with FDR correction was performed. Fig. 5E and S7

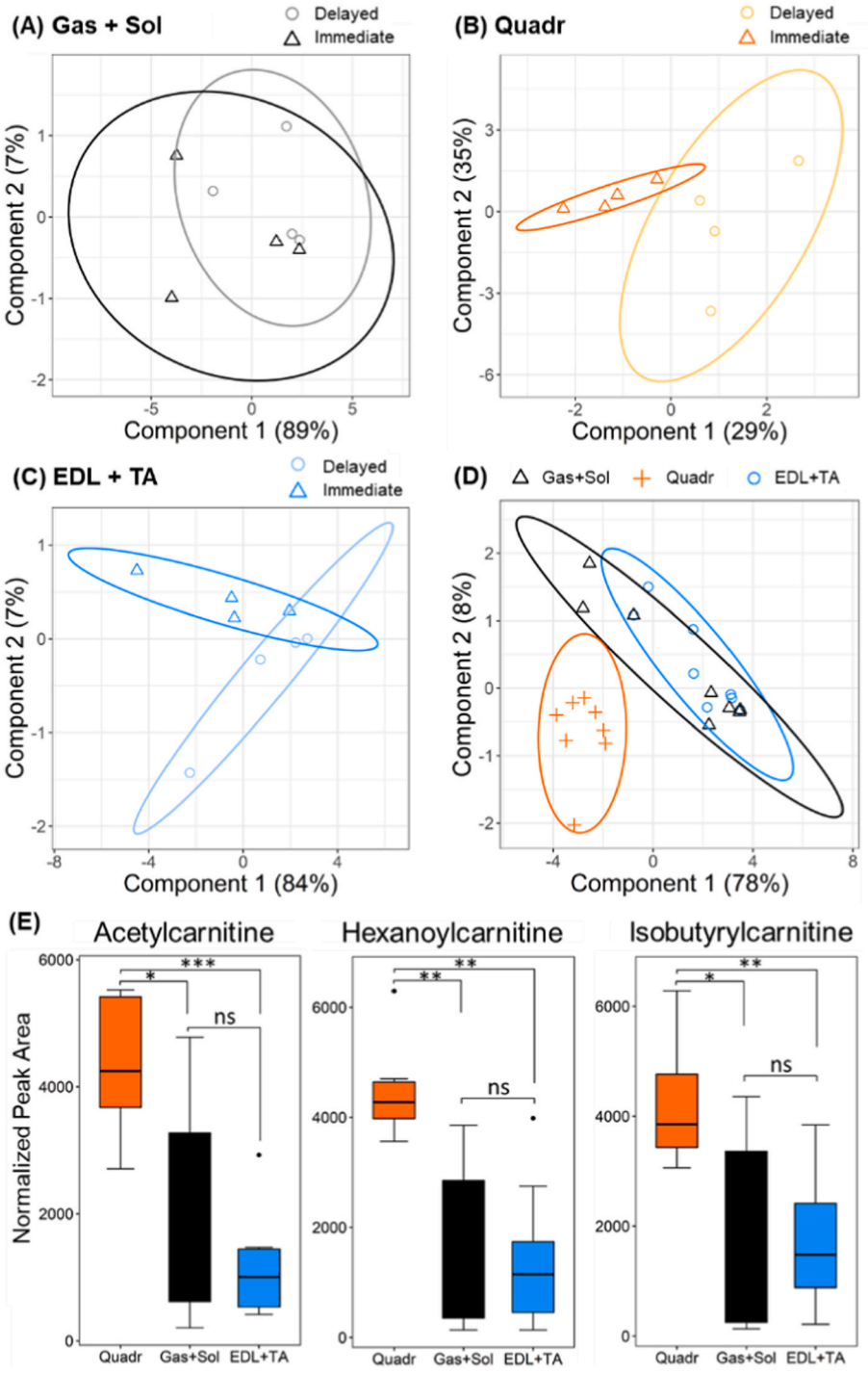

Fig. 5. The PLS-DA score plots illustrate the effects of muscle tissue isolation speed on acylcarnitine stability across three muscle tissue types: Gas + Sol (A), Quadr (B), and EDL + TA (C) (n = 4). The overall PLS-DA score plot (D) and *t*-test results with FDR correction (E) for three representative acylcarnitines in these muscle tissues are presented (n = 8). The complete *t*-test results for all acylcarnitines can be found in Fig. S7. *$p < 0.05$, **$p < 0.01$, ***$p < 0.001$. ns means no significant difference.

revealed significantly higher acylcarnitine levels in Quadr than in Gas + Sol. This may be attributed to the inclusion of type-I oxidative muscle (soleus) in Gas + Sol and the predominantly type-II glycolytic nature of Quadr [59]. The greater presence of fatty acid transporters in oxidative muscles compared to glycolytic muscles likely contributes to the lower acylcarnitine abundance in oxidative muscle [60]. Similar findings have been reported by Warren et al. and Bonen et al. [60,61]. Although both Quadr and EDL are classified as glycolytic muscles, EDL + TA showed significantly lower acylcarnitine levels (Fig. 5 and S7). This discrepancy may result from the considerable variation in muscle type composition and fiber density within EDL and TA, as well as individual differences [62]. Additionally, in *Ercc1*$^{\Delta/-}$ mice, the fiber composition of EDL muscle differs from that of wild-type controls, with reduced type IIA/IIX fibers and an increased proportion of type IIB fibers [30].

4. Conclusion

A fully automated, high-throughput electro-extraction (EE) platform was developed by integrating hardware components—a custom-designed 96-well plate with a built-in bottom electrode, a high-voltage power supply, a CTC PAL3 autosampler, and an LC-MS analyzer—along with software for system control. A Design of Experiment (DoE) approach using a Box-Behnken design was employed to optimize the platform's parameters. The optimized EE setup was successfully applied to human plasma samples, achieving LODs as low as 3.0 pg mL^{-1}, and was subsequently successfully used to investigate acylcarnitine abundance in various muscle types and their stability in progeroid (*Ercc1*$^{\Delta/-}$) mouse muscle tissues.

In summary, this study presents a stable and robust automated EE platform that can be directly coupled to LC-MS for high-throughput biofluid and -tissue analysis, particularly for low-volume, low-concentration samples. Around 120 samples can be extracted and analyzed per day by the workflow for acylcarnitines, with a cost of less than 0.1 Euro per sample. The throughput can be further increased, and costs reduced by shortening the electro-extraction time and minimizing solvent consumption. This technique holds immense potential for steering the evolution of comprehensive automated and high-throughput bioanalytic workflows in the future.

CRediT authorship contribution statement

Yupeng He: Writing – review & editing, Writing – original draft, Validation, Project administration, Methodology, Formal analysis, Data curation, Conceptualization. **Paul Miggiels:** Writing – review & editing, Software. **Amy Harms:** Writing – review & editing, Methodology. **Yvonne Rijksen:** Resources. **Renata M.C. Brandt:** Resources. **Wilbert P. Vermeij:** Writing – review & editing, Resources. **Bert Wouters:** Writing – review & editing, Supervision, Methodology. **Thomas Hankemeier:** Supervision, Funding acquisition.

Declaration of competing interest

The authors declare that they have no known competing financial interests or personal relationships that could have appeared to influence the work reported in this paper.

Acknowledgments

The authors are grateful to Emiel Wiegers and Raphaël Zwier from the Fine Mechanical Department (FMD) at Leiden University for their contribution in developing, modifying, and manufacturing of the 96-well plate and its bottom electrode. We thank Tom Vercammen and Inge De Dobbeleer from Interscience for discussions and suggestions during the development and integration of the electro-extraction setup in the CTC PAL autosampler. Kimberly Smit, Sander Barnhoorn, Yvette van Loon, and the animal caretakers are acknowledged for general assistance with mouse experiments. We thank Jan Hoeijmakers for valuable discussions and advice. This work was supported by the Netherlands Organisation for Scientific Research (NWO) in the Building Blocks of Life (grant number 737.016.015). This research was (partially) funded by the X-Omics project (Netherlands Organisation for Scientific Research, project No. 184.034.019) and MOONLIGHT project (Netherlands Organisation for Scientific Research, grant number ENPPS. TA.019.004).

Appendix A. Supplementary data

Supplementary data to this article can be found online at https://doi.org/10.1016/j.aca.2025.344224.

Data availability

Data will be made available on request.

References

[1] L.G. Blomberg, Two new techniques for sample preparation in bioanalysis: microextraction in packed sorbent (MEPS) and use of a bonded monolith as sorbent for sample preparation in polypropylene tips for 96-well plates, Anal. Bioanal. Chem. 393 (2009) 797–807, https://doi.org/10.1007/s00216-008-2305-4.
[2] J. Henion, E. Brewer, G. Rule, Sample preparation for LC/MS/MS: analyzing biological and environmental samples, Anal. Chem. 70 (1998) 650a–656a, https://doi.org/10.1021/ac981991q.
[3] R.N.X. Xu, L.M. Fan, M.J. Rieser, T.A. El-Shourbagy, Recent advances in high-throughput quantitative bioanalysis by LC-MS/MS, J. Pharm. Biomed. 44 (2007) 342–355, https://doi.org/10.1016/j.jpba.2007.02.006.
[4] R.J. Raterink, P.W. Lindenburg, R.J. Vreeken, R. Ramautar, T. Hankemeier, Recent developments in sample-pretreatment techniques for mass spectrometry-based metabolomics, Trac. Trends Anal. Chem. 61 (2014) 157–167, https://doi.org/10.1016/j.trac.2014.06.003.
[5] M.A. Dineva, L. Mahilum-Tapay, H. Lee, Sample preparation: a challenge in the development of point-of-care nucleic acidbased assays for resource-limited settings, Analyst 132 (2007) 1193–1199, https://doi.org/10.1039/b705672a.
[6] S.X. Peng, M. Cousineau, S.J. Juzwin, D.M. Ritchie, A 96-well screen filter plate for high-throughput biological sample preparation and LC-MS/MS analysis, Anal. Chem. 78 (2006) 343–348, https://doi.org/10.1021/ac051514p.
[7] D. Vuckovic, Current trends and challenges in sample preparation for global metabolomics using liquid chromatography-mass spectrometry, Anal. Bioanal. Chem. 403 (2012) 1523–1548, https://doi.org/10.1007/s00216-012-6039-y.
[8] P. Miggiels, B. Wouters, G.J.P. van Westen, A.C. Dubbelman, T. Hankemeier, Novel technologies for metabolomics: more for less, Trac. Trends Anal. Chem. 120 (2019) 115323, https://doi.org/10.1016/j.trac.2018.11.021.
[9] I. Kohler, J. Schappler, S. Rudaz, Microextraction techniques combined with capillary electrophoresis in bioanalysis, Anal. Bioanal. Chem. 405 (2013) 125–141, https://doi.org/10.1007/s00216-012-6367-y.
[10] A. Oedit, B. Duivelshof, P.W. Lindenburg, T. Hankemeier, Integration of three-phase microelectroextraction sample preparation into capillary electrophoresis, J. Chromatogr. A 1610 (2020) 460570, https://doi.org/10.1016/j.chroma.2019.460570.
[11] A. Sarafraz-Yazdi, A. Amiri, Liquid-phase microextraction, Trac. Trends Anal. Chem. 29 (2010) 1–14, https://doi.org/10.1016/j.trac.2009.10.003.
[12] D.E. Raynie, Modern extraction techniques, Anal. Chem. 82 (2010) 4911–4916, https://doi.org/10.1021/ac101223c.
[13] Y.Y. Wen, L. Chen, J.H. Li, D.Y. Liu, L.X. Chen, Recent advances in solid-phase sorbents for sample preparation prior to chromatographic analysis, Trac. Trends Anal. Chem. 59 (2014) 26–41, https://doi.org/10.1016/j.trac.2014.03.011.
[14] A.Y. Song, J. Yang, Efficient determination of amphetamine and methylamphetamine in human urine using electro-enhanced single-drop microextraction with in-drop derivatization and gas chromatography, Anal. Chim. Acta 1045 (2019) 162–168, https://doi.org/10.1016/j.aca.2018.09.024.
[15] A. Oedit, R. Ramautar, T. Hankemeier, P.W. Lindenburg, Electroextraction and electromembrane extraction: advances in hyphenation to analytical techniques, Electrophoresis 37 (2016) 1170–1186, https://doi.org/10.1002/elps.201500530.
[16] P.W. Lindenburg, R. Ramautar, T. Hankemeier, The potential of electrophoretic sample pretreatment techniques and new instrumentation for bioanalysis, with a focus on peptidomics and metabolomics, Bioanalysis 5 (2013) 2785–2801, https://doi.org/10.4155/bio.13.254.
[17] N. Drouin, P. Kuban, S. Rudaz, S. Pedersen-Bjergaard, J. Schappler, Electromembrane extraction: overview of the last decade, Trac. Trends Anal. Chem. 113 (2019) 357–363, https://doi.org/10.1016/j.trac.2018.10.024.
[18] R.J. Raterink, P.W. Lindenburg, R.J. Vreeken, T. Hankemeier, Three-phase electroextraction: a new (online) sample purification and enrichment method for bioanalysis, Anal. Chem. 85 (2013) 7762–7768, https://doi.org/10.1021/ac4010716.
[19] Y. He, P. Miggiels, N. Drouin, P.W. Lindenburg, B. Wouters, T. Hankemeier, An automated online three-phase electro-extraction setup with machine-vision process

monitoring hyphenated to LC-MS analysis, Anal. Chim. Acta 1235 (2022) 340521, https://doi.org/10.1016/j.aca.2022.340521.
[20] V. Santilli, A. Bernetti, M. Mangone, M. Paoloni, Clinical definition of sarcopenia, Clin Cases Miner Bone Meta 11 (2014) 177–180.
[21] R.A. Fielding, B. Vellas, W.J. Evans, S. Bhasin, J.E. Morley, A.B. Newman, G. Abellan van Kan, S. Andrieu, J. Bauer, D. Breuille, T. Cederholm, J. Chandler, C. De Meynard, L. Donini, T. Harris, A. Kannt, F. Keime Guibert, G. Onder, D. Papanicolaou, Y. Rolland, D. Rooks, C. Sieber, E. Souhami, S. Verlaan, M. Zamboni, Sarcopenia: an undiagnosed condition in older adults. Current consensus definition: prevalence, etiology, and consequences. International working group on sarcopenia, J. Am. Med. Dir. Assoc. 12 (2011) 249–256, https://doi.org/10.1016/j.jamda.2011.01.003.
[22] W.P. Vermeij, J.H. Hoeijmakers, J. Pothof, Genome integrity in aging: human syndromes, mouse models, and therapeutic options, Annu. Rev. Pharmacol. Toxicol. 56 (2016) 427–445, https://doi.org/10.1146/annurev-pharmtox-010814-124316.
[23] M.E. Dolle, R.V. Kuiper, M. Roodbergen, J. Robinson, S. de Vlugt, S.W. Wijnhoven, R.B. Beems, L. de la Fonteyne, P. de With, I. van der Pluijm, L.J. Niedernhofer, P. Hasty, J. Vijg, J.H. Hoeijmakers, H. van Steeg, Broad segmental progeroid changes in short-lived Ercc1(-/Delta7) mice, Pathobiol Aging Age Relat Dis 1 (2011), https://doi.org/10.3402/pba.v1i0.7219.
[24] G. Weeda, I. Donker, J. de Wit, H. Morreau, R. Janssens, C.J. Vissers, A. Nigg, H. van Steeg, D. Bootsma, J.H. Hoeijmakers, Disruption of mouse ERCC1 results in a novel repair syndrome with growth failure, nuclear abnormalities and senescence, Curr. Biol. 7 (1997) 427–439, https://doi.org/10.1016/s0960-9822(06)00190-4.
[25] L.J. Niedernhofer, G.A. Garinis, A. Raams, A.S. Lalai, A.R. Robinson, E. Appeldoorn, H. Odijk, R. Oostendorp, A. Ahmad, W. Van Leeuwen, A new progeroid syndrome reveals that genotoxic stress suppresses the somatotroph axis, Nature 444 (2006) 1038–1043, https://doi.org/10.1038/nature05456.
[26] C. Milanese, C.R. Bombardieri, S. Sepe, S. Barnhoorn, C. Payán-Goméz, D. Caruso, M. Audano, S. Pedretti, W.P. Vermeij, R.M.C. Brandt, A. Gyenis, M.M. Wamelink, A.S. de Wit, R.C. Janssens, R. Leen, A.B.P. van Kuilenburg, N. Mitro, J. H. Hoeijmakers, P.G. Mastroberardino, DNA damage and transcription stress cause ATP-Mediated redesign of metabolism and potentiation of anti-oxidant buffering, Nat. Commun. 1 (2019) 4887, https://doi.org/10.1038/s41467-019-12640-5.
[27] A. Gyenis, J. Chang, J.G. Demmers, S.T. Bruens, S. Barnhoorn, R.C. Brandt, M. P. Baar, M. Raseta, K.L. Derks, J.H. Hoeijmakers, J. Pothof, Genome-wide RNA polymerase stalling shapes the transcriptome during aging, Nat. Genet. 2 (2023) 268–279, https://doi.org/10.1038/s41588-022-01279-6.
[28] E.L. de Graaf, W.P. Vermeij, M.C. de Waard, Y. Rijksen, I. van der Pluijm, C. C. Hoogenraad, J.H. Hoeijmakers, A.F. Altelaar, A.J. Heck, Spatio-temporal analysis of molecular determinants of neuronal degeneration in the aging mouse cerebellum, Mol. Cell. Proteomics 12 (2013) 1350–1362, https://doi.org/10.1074/mcp.M112.024950.
[29] M.J. Yousefzadeh, J. Zhao, C. Bukata, E.A. Wade, S.J. McGowan, L.A. Angelini, M. P. Bank, A.U. Gurkar, C.A. McGuckian, M.F. Calubag, J.I. Kato, C.E. Burd, P. D. Robbins, L.J. Niedernhofer, Tissue specificity of senescent cell accumulation during physiologic and accelerated aging of mice, Aging Cell 19 (2020) e13094, https://doi.org/10.1111/acel.13094.
[30] K. Alyodawi, W.P. Vermeij, S. Omairi, O. Kretz, M. Hopkinson, F. Solagna, B. Joch, R.M.C. Brandt, S. Barnhoorn, N. van Vliet, Y. Ridwan, J. Essers, R. Mitchell, T. Morash, A. Pasternack, O. Ritvos, A. Matsakas, H. Collins-Hooper, T.B. Huber, J. H. Hoeijmakers, K. Patel, Compression of morbidity in a progeroid mouse model through the attenuation of myostatin/activin signalling, J Cachexia Sarcopenia Muscle 10 (2019) 662–686, https://doi.org/10.1002/jcsm.12404.
[31] W.P. Vermeij, M.E.T. Dollé, E. Reiling, D. Jaarsma, C. Payan-Gomez, C. R. Bombardieri, H. Wu, A.J.M. Roks, S.M. Botter, B.C. van der Eerden, S.A. Youssef, R.V. Kuiper, B. Nagarajah, C.T. van Oostrom, R.M.C. Brandt, S. Barnhoorn, S. Imholz, J.L.A. Pennings, A. de Bruin, Á. Gyenis, J. Pothof, J. Vijg, H. van Steeg, J. H.J. Hoeijmakers, Restricted diet delays accelerated ageing and genomic stress in DNA-repair-deficient mice, Nature 537 (2016) 427–431, https://doi.org/10.1038/nature19329.
[32] M.B. Birkisdóttir, L.J. Van't Sant, R.M.C. Brandt, S. Barnhoorn, J.H.J. Hoeijmakers, W.P. Vermeij, D. Jaarsma, Purkinje-cell-specific DNA repair-deficient mice reveal that dietary restriction protects neurons by cell-intrinsic preservation of genomic health, Front. Aging Neurosci. 14 (2022) 1095801, https://doi.org/10.3389/fnagi.2022.1095801.
[33] Y. Yang, C. Cruickshank, M. Armstrong, S. Mahaffey, R. Reisdorph, N. Reisdorph, New sample preparation approach for mass spectrometry-based profiling of plasma results in improved coverage of metabolome, J. Chromatogr. A 1300 (2013) 217–226, https://doi.org/10.1016/j.chroma.2013.04.030.
[34] R.D.A.M. Alves, A.D. Dane, A. Harms, K. Strassburg, R.M. Seifar, L.B. Verdijk, S. Kersten, R. Berger, T. Hankemeier, R.J. Vreeken, Global profiling of the muscle metabolome: method optimization, validation and application to determine exercise-induced metabolic effects, Metabolomics 11 (2014) 271–285, https://doi.org/10.1007/s11306-014-0701-7.
[35] Y. He, P. Miggiels, B. Wouters, N. Drouin, F. Guled, T. Hankemeier, P. W. Lindenburg, A high-throughput, ultrafast, and online three-phase electro-extraction method for analysis of trace level pharmaceuticals, Anal. Chim. Acta 1149 (2021) 338204, https://doi.org/10.1016/j.aca.2021.338204.
[36] N. Drouin, S. Rudaz, J. Schappler, Dynamic-electromembrane extraction: a technical development for the extraction of neuropeptides, Anal. Chem. 88 (2016) 5308–5315, https://doi.org/10.1021/acs.analchem.6b00559.
[37] D.R. Mani, S.E. Abbatiello, S.A. Carr, Statistical characterization of multiple-reaction monitoring mass spectrometry (MRM-MS) assays for quantitative proteomics, BMC Bioinf. 13 (2012) S9, https://doi.org/10.1186/1471-2105-13-S16-S9.
[38] F.A. Hansen, P. Kuban, E.L. Oiestad, S. Pedersen-Bjergaard, Electromembrane extraction of highly polar bases from biological samples - deeper insight into bis(2-ethylhexyl) phosphate as ionic carrier, Anal. Chim. Acta 1115 (2020) 23–32, https://doi.org/10.1016/j.aca.2020.04.027.
[39] N. Drouin, J.F. Mandscheff, S. Rudaz, J. Schappler, Development of a new extraction device based on parallel-electromembrane extraction, Anal. Chem. 89 (2017) 6346–6350, https://doi.org/10.1021/acs.analchem.7b01284.
[40] T.M. Middelthon-Bruer, A. Gjelstad, K.E. Rasmussen, S. Pedersen-Bjergaard, Parameters affecting electro membrane extraction of basic drugs, J. Sep. Sci. 31 (2008) 753–759, https://doi.org/10.1002/jssc.200700502.
[41] S. Seidi, Y. Yamini, M. Rezazadeh, Electrically enhanced microextraction for highly selective transport of three β-blocker drugs, J. Pharm. Biomed. Anal. 56 (2011) 859–866, https://doi.org/10.1016/j.jpba.2011.07.029.
[42] A. Gjelstad, K.E. Rasmussen, S. Pedersen-Bjergaard, Simulation of flux during electro-membrane extraction based on the nernst-planck equation, J. Chromatogr. A 1174 (2007) 104–111, https://doi.org/10.1016/j.chroma.2007.08.057.
[43] L.E.E. Eibak, A. Gjelstad, K.E. Rasmussen, S. Pedersen-Bjergaard, Kinetic electro membrane extraction under stagnant conditions-fast isolation of drugs from untreated human plasma, J. Chromatogr. A 1217 (2010) 5050–5056, https://doi.org/10.1016/j.chroma.2010.06.018.
[44] K.S. Hasheminasab, A.R. Fakhari, A. Shahsavani, H. Ahmar, A new method for the enhancement of electromembrane extraction efficiency using carbon nanotube reinforced hollow fiber for the determination of acidic drugs in spiked plasma, urine, breast milk and wastewater samples, J. Chromatogr. A 1285 (2013) 1–6, https://doi.org/10.1016/j.chroma.2013.01.115.
[45] M. Balchen, A. Gjelstad, K.E. Rasmussen, S. Pedersen-Bjergaard, Electrokinetic migration of acidic drugs across a supported liquid membrane, J. Chromatogr. A 1152 (2007) 220–225, https://doi.org/10.1016/j.chroma.2006.10.096.
[46] S. Nojavan, A. Pourahadi, S.S. Hosseiny Davarani, A. Morteza-Najarian, M. Beigzadeh Abbassi, Electromembrane extraction of zwitterionic compounds as acid or base: Comparison of extraction behavior at acidic and basic pHs, Anal. Chim. Acta 745 (2012) 45–52, https://doi.org/10.1016/j.aca.2012.07.044.
[47] A. Slampova, P. Kuban, P. Bocek, Quantitative aspects of electrolysis in electromembrane extractions of acidic and basic analytes, Anal. Chim. Acta 887 (2015) 92–100, https://doi.org/10.1016/j.aca.2015.06.040.
[48] J.W. Schoonen, V. van Duinen, A. Oedit, P. Vulto, T. Hankemeier, P. W. Lindenburg, Continuous-flow microelectroextraction for enrichment of low abundant compounds, Anal. Chem. 86 (2014) 8048–8056, https://doi.org/10.1021/ac500707v.
[49] S. Nojavan, S. Asadi, Electromembrane extraction using two separate cells: a new design for simultaneous extraction of acidic and basic compounds, Electrophoresis 37 (2016) 587–594, https://doi.org/10.1002/elps.201500455.
[50] C.X. Huang, A. Gjelstad, S. Pedersen-Bjergaard, Electromembrane extraction with alkylated phosphites and phosphates as supported liquid membranes, J. Membr. Sci. 526 (2017) 18–24, https://doi.org/10.1016/j.memsci.2016.11.049.
[51] C.X. Huang, K.F. Seip, A. Gjelstad, S. Pedersen-Bjergaard, Electromembrane extraction of polar basic drugs from plasma with pure bis(2-ethylhexyl) phosphite as supported liquid membrane, Anal. Chim. Acta 934 (2016) 80–87, https://doi.org/10.1016/j.aca.2016.06.002.
[52] Y. He, N. Drouin, B. Wouters, P. Miggiels, T. Hankemeier, P.W. Lindenburg, Development of a fast, online three-phase electroextraction hyphenated to fast liquid chromatography–mass spectrometry for analysis of trace-level acid pharmaceuticals in plasma, Anal. Chim. Acta 1192 (2022) 339364, https://doi.org/10.1016/j.aca.2021.339364.
[53] C. Li, Y. Yan, C. Hong, X. Wei, J. Xiong, C. Huang, X. Shen, Successive electromembrane extraction: a new insight in simultaneous extraction of polar and non-polar metabolic molecules from biological samples, Anal. Chim. Acta (2025) 343727, https://doi.org/10.1016/j.aca.2025.343727.
[54] P.W. Lindenburg, U.R. Tjaden, J.V.D. Greef, T. Hankemeier, Feasibility of electroextraction as versatile sample preconcentration for fast and sensitive analysis of urine metabolites, demonstrated on acylcarnitines, Electrophoresis 33 (2012) 2987–2995, https://doi.org/10.1002/elps.201200276.
[55] M. Réjane, M. Donzelli, M. Haschke, S. Krähenbühl, Quantification of plasma carnitine and acylcarnitines by high-performance liquid chromatography-tandem mass spectrometry using online solid-phase extraction, Anal. Bioanal. Chem. 405 (2013) 8829–8836, https://doi.org/10.1007/s00216-013-7309-z.
[56] M. Sylwia, J. Baranowski, Determination of carnitine and acylcarnitines in human urine by means of microextraction in packed sorbent and hydrophilic interaction chromatography–ultra-high-performance liquid chromatography–tandem mass spectrometry, J. Pharm. Biomed. Anal. 109 (2015) 171–176, https://doi.org/10.1016/j.jpba.2015.02.044.
[57] K.S. Babu, J.K. Amamcharla, Rehydration characteristics of milk protein concentrate powders monitored by electrical resistance tomography, JDS Communications 2 (2021) 313–318, https://doi.org/10.3168/jdsc.2021-0125.
[58] Y. Zhang, H. Jiang, P. Hutson, Stability of acetyl-1-carnitine in 5% dextrose using a high-performance liquid chromatography-mass spectrometry times 2 method, Int. J. Pharm. Compd. 16 (2012) 170–173.
[59] R.A. Jacobs, V. Díaz, L. Soldini, T. Haider, M. Thomassen, N.B. Nordsborg, M. Gassmann, C. Lundby, Fast-twitch glycolytic skeletal muscle is predisposed to age-induced impairments in mitochondrial function, J. Gerontol. A Biol. Sci. Med. Sci. 9 (2013) 1010–1022, https://doi.org/10.1093/gerona/gls335.
[60] A. Bonen, J.J.F.P. Luiken, S. Liu, D.J. Dyck, B. Kiens, S. Kristiansen, L.P. Turcotte, G.J. Van Der Vusse, J.F.C. Glatz, Palmitate transport and fatty acid transporters in

red and white muscles, Am. J. Physiol. Endocrinol. Metab. 3 (1998) E471–E478, https://doi.org/10.1152/ajpendo.1998.275.3.E471.
[61] B.E. Warren, P.H. Lou, E. Lucchinetti, L. Zhang, A.S. Clanachan, A. Affolter, M. Hersberger, M. Zaugg, H. Lemieux, Early mitochondrial dysfunction in glycolytic muscle, but not oxidative muscle, of the fructose-fed insulin-resistant rat, Am. J. Physiol. Endocrinol. Metab. 6 (2014) E658–E667, https://doi.org/10.1152/ajpendo.00511.2013.
[62] J. Lexell, J.C. Jarvis, J. Currie, D.Y. Downham, S. Salmons, Fibre type composition of rabbit tibialis anterior and extensor digitorum longus muscles, J. Anat. 185 (1994) 95.